J|A|C|S
ARTICLES
Published on Web 03/21/2006

Dynamics and Mechanism of Bridge-Dependent Charge Separation in Pyrenylurea−Nitrobenzene π-Stacked Protophanes

Frederick D. Lewis,*,† Pierre Daublain,† Grace B. Delos Santos,† Weizhong Liu,† Arpine M. Asatryan,§ Shriaz A. Markarian,*,§ Torsten Fiebig,*,‡ Milen Raytchev,‡ and Qiang Wang‡

Contribution from the Departments of Chemistry, Northwestern University, Evanston, Illinois 60208, Yerevan State University, 375049 Yerevan, Armenia, and Boston College, Chestnut Hill, Massachusetts 02467

Received December 6, 2005; E-mail: lewis@chem.northwestern.edu; shmarkar@ysu.am; fiebig@bc.edu

Abstract: Herein are reported the synthesis, structure, and electronic properties of a series of tertiary di- and polyarylureas possessing pyrene and nitrobenzene end groups separated by a variable number of internal phenylenediamine bridging groups. These molecules adopt folded "protophane" structures in which the adjacent arenes are loosely π-stacked. The behavior of both the pyrene and nitrobenzene singlet states has been investigated by means of femtosecond broadband pump−probe spectroscopy, and the transients have been assigned on the basis of comparison to reference molecules. Femtosecond time resolution permits direct observation of the fast internal conversion process for both the pyrene and nitrobenzene upper singlet states, as well as the intersystem crossing of nitrobenzene. The ultrafast (ca. 100 fs) charge separation of the donor−acceptor urea having no bridging group is attributed to an internal conversion process. The slower charge separation and charge recombination of the donor−acceptor urea having a single bridging group occur via a bridge-mediated superexchange process. Addition of a second bridging unit results in a role reversal for the pyrene singlet state, which now serves as an excited-state acceptor with the bridging units serving as the electron donors. The change in the directionality of electron transfer upon addition of a second bridging phenylenediamine is a consequence of a decrease in the bridge oxidation potential as well as a decrease in the rate constant for single-step superexchange electron transfer.

Introduction

The mechanism and dynamics of photoinduced intramolecular electron transfer processes between aromatic chromophores in donor−bridge−acceptor systems have been extensively investigated.[1] Both single-step superexchange and multistep hopping mechanisms have been identified.[2] The former is expected to display a pronounced exponential decrease in rate as the donor−acceptor distance is increased, whereas the latter can display a much softer distance dependence.[3] Most investigations of bridge-mediated electron transfer reported to date have employed linear systems having extended geometries.[4] However, there is growing interest in both natural and synthetic π-stacked systems. The former include the light-harvesting antennae and reaction centers of photosynthetic bacteria and green plants[5] as well as the π-stacked base pairs of duplex DNA.[6] Our recent studies of electron-transfer dynamics in DNA-capped hairpin systems have shown that photoinduced charged separation occurs via a superexchange mechanism when one or two base pairs separate the donor and acceptor and via a hopping mechanism at longer distances.[7]

Examples of synthetic π-stacked donor−bridge−acceptor systems include donor−acceptor systems possessing a cleft that can accommodate either an aromatic solvent or a covalently attached aromatic bridge,[8] multilayered cyclophanes,[9] and singly linked "protophanes" assembled with 1,8-diarylnaphthalene scaffolds.[10,11] Therien and co-workers have investigated the dynamics of photoinduced electron transfer in π-stacked systems having a porphyrin donor separated from a quinone acceptor

† Northwestern University.
§ Yerevan State University.
‡ Boston College.

(1) Paddon-Row, M. N. In *Electron Transfer in Chemistry*; Balzani, V., Ed.; Wiley-VCH: Weinheim, 2001; Vol. 3, pp 179−271.
(2) Weiss, E. A.; Tauber, M. J.; Kelley, R. F.; Ahrens, M. J.; Ratner, M. A.; Wasielewski, M. R. *J. Am. Chem. Soc.* **2005**, *127*, 11842−11850.
(3) (a) Felts, A. K.; Pollard, W. T.; Friesner, R. A. *J. Phys. Chem.* **1995**, *99*, 2929−2940. (b) Jortner, J.; Bixon, M.; Langenbacher, T.; Michel-Beyerle, M. E. *Proc. Natl. Acad. Sci. U.S.A.* **1998**, *95*, 12759−12765.
(4) Wasielewski, M. R. *Chem. Rev.* **1992**, *92*, 435−461.
(5) Moser, C. C.; Page, C. C.; Dutton, L. P. In *Electron Transfer in Chemistry*; Balzani, V., Ed.; Wiley-VCH: Weinheim, 2001; Vol. 3, pp 24−38.
(6) Lewis, F. D.; Wu, Y. *J. Photochem. Photobiol. C: Rev.* **2001**, *2*, 1−16.
(7) Lewis, F. D.; Zhu, H.; Daublain, P.; Fiebig, T.; Raytchev, M.; Wang, Q.; Shafirovich, V. *J. Am. Chem. Soc.* **2006**, *128*, 791−800.
(8) (a) Napper, A. M.; Read, I.; Waldeck, D. H.; Head, N. J.; Oliver, A. M.; Paddon-Row, M. N. *J. Am. Chem. Soc.* **2000**, *122*, 5220−5221. (b) Zimmt, M. B.; Waldeck, D. H. *J. Phys. Chem. A* **2003**, *107*, 3580−3597.
(9) (a) Machida, H.; Tatemitsu, H.; Otsubo, T.; Sakata, Y.; Misumi, S. *Bull. Chem. Soc. Jpn.* **1980**, *53*, 2943−2952. (b) Vögtle, F. *Cyclophane Chemistry: Synthesis, Structures, and Reactions*; J. Wiley: Chichester/New York, 1993.
(10) Kang, Y. K.; Rubtsov, I. V.; Iovine, P. M.; Chen, J.; Therien, M. J. *J. Am. Chem. Soc.* **2002**, *124*, 8275−8279.
(11) Rubtsov, I. V.; Kang, Y. K.; Redmore, N. P.; Allen, R. M.; Zheng, J.; Beratan, D. N.; Therien, M. J. *J. Am. Chem. Soc.* **2004**, *126*, 5022−5023.

10.1021/ja058050x CCC: $33.50

Chart 1. Structures of Ureas **1**−**7** Shown with Flattened Two-Dimensional Geometries

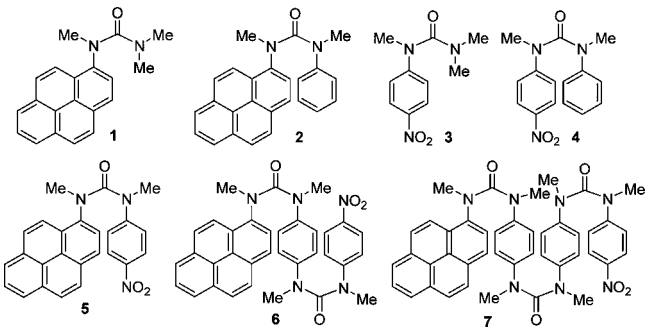

by 0−2 bridging phenyls using 1,8-diarylnaphthalenes as the bridging units.[10] They observe faster rate constants for charge separation and charge recombination and a softer distance dependence for the rates of both processes than the corresponding values for donor−acceptor systems with bridging DNA base pairs.[7,12]

Our interest in electron-transfer processes in DNA led us to explore synthetic π-stacked donor−bridge−acceptor systems which are soluble in organic solvents. This property would permit investigation of the solvent and temperature dependence of charge separation and charge recombination. Aromatic systems assembled with tertiary urea linkers were selected for these studies on the basis of their formation of strain-free folded conformations and the relative ease and flexibility of the synthetic methods for their preparation.[13] We have previously reported that *N*,*N*′-diaryl-*N*,*N*′-dimethylureas can form intramolecular excimers, exciplexes, or ion pairs, depending upon the choice of aromatic components.[14−16] We have also reported methods for the assembly of multilayer systems in which internal phenylenediamines serve as π-bridges separating the external arenes.[17,18]

We report here the use of femtosecond broadband pump−probe spectroscopy to study the dynamics of charge separation and charge recombination in a series of polyarylureas having pyrene and nitrobenzene end groups separated by zero, one, or two bridging phenylenediamines (Chart 1). The high temporal and spectral resolution of these experiments permits a direct observation and characterization of the underlying photophysical processes (i.e., internal conversion, intersystem crossing, electron and hole transfer) which contribute to the overall excited-state quenching. Markedly different behavior is observed for the three members of this series. Charge separation occurs for the system lacking a bridging unit via an ultrafast internal conversion mechanism and for the system possessing a single bridging unit by a slower superexchange process. Insertion of a second bridging unit results in a change in the directionality of electron transfer from electron injection to hole injection into the bridge.

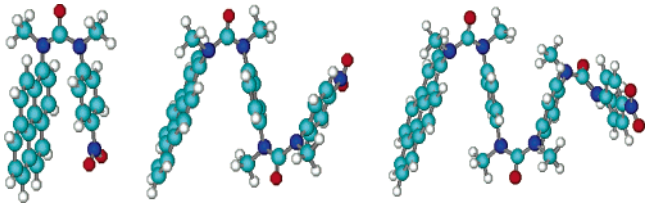

Figure 1. AM1-minimized structures for ureas **5**, **6**, and **7**.

Results

Synthesis and Structure. The syntheses of the ureas **1**−**4** (Chart 1) by means of *N*-methylation of the corresponding secondary ureas have been reported.[16,18] The pyrene−nitrobenzene (Py-NB) ureas **5**−**7** were prepared using the procedures employed for structurally related naphthylureas (see Experimental Section).[17] The arylureas were purified by column chromatography and characterized by means of ^{1}H NMR, mass spectra, and elemental analysis.

The gas-phase geometries of the arylureas were optimized using the semiempirical AM1 method, which provides reliable estimated geometries for organic molecules.[19] Calculated minima for the tertiary ureas have folded structures, as shown in Figure 1 for **5**−**7**. Rotation about the pyrene−urea bond produces two minima of equal energy. Folded structures with E arylurea conformations are typically several kilocalories per mol more stable than extended structures for these tertiary ureas, as is the case for other tertiary di- and polyarylureas.[15] The preference for folded geometries is largely steric in origin, the steric repulsion between two methyl groups or one aryl and one phenyl being larger than those for two aryl groups, which can adopt face-to-face structures.

The ^{1}H NMR spectra (Experimental Section) of the tertiary ureas provide additional evidence for folded structures in solution. The phenyl protons in **2** and nitrophenyl protons in **4**−**7** are shifted upfield when compared to those of **3** or of the corresponding secondary ureas. Large upfield shifts are also observed for the protons of the bridging phenylenediamine rings of **6** and **7**. The upfield shifts are larger than those previously observed for the analogous naphthylureas as a consequence of the larger π-surface of pyrene.[17]

Absorption Spectra. The absorption spectra of the arylureas **2** and **4**−**7** are shown in Figure 2, and the band maxima and molar absorbance of ureas **1**−**7** are summarized in Table 1. The spectra of **1** and **2** have previously been reported and are similar in band shape to the spectrum of pyrene.[16] The weak shoulder at 380 nm corresponds to pyrene band 1, whereas the stronger 348 nm band corresponds to pyrene band 2.[20] The broad, long-wavelength band of urea **4** has been assigned to a nitrobenzene-localized $\pi-\pi^*$ transition.[18] The spectra of ureas **5**−**7** approximate the sum of the absorption spectra of **2** and **4**. The bandwidth increases as the number of aryl groups increases for **5**−**7**.

Further information concerning the absorption spectra is provided by the semiempirical Hartree−Fock intermediate neglect of differential overlap (INDO) method as parametrized by Zerner and co-workers (ZINDO)[21] and implemented in

(12) Lewis, F. D.; Wu, Y.; Zhang, L.; Zuo, X.; Hayes, R. T.; Wasielewski, M. R. *J. Am. Chem. Soc.* **2004**, *126*, 8206−8215.
(13) (a) Yamaguchi, K.; Matsumura, G.; Kagechika, H.; Azumaya, I.; Ito, Y.; Itai, A.; Shudo, K. *J. Am. Chem. Soc.* **1991**, *113*, 5474−5475. (b) Krebs, F. C.; Jorgensen, M. *J. Org. Chem.* **2002**, *67*, 7511−7518.
(14) Lewis, F. D.; Kurth, T. L.; Liu, W. *Photochem. Photobiol. Sci.* **2002**, *1*, 30−37.
(15) Kurth, T. L.; Lewis, F. D. *J. Am. Chem. Soc.* **2003**, *125*, 13760−13767.
(16) Lewis, F. D.; Kurth, T. L. *Can. J. Chem.* **2003**, *81*, 770−776.
(17) Delos Santos, G. B.; Lewis, F. D. *J. Phys. Chem. A* **2005**, *109*, 8106−8112.
(18) Lewis, F. D.; Delos Santos, G. B.; Liu, W. *J. Org. Chem.* **2005**, *70*, 2974−2979.
(19) *CAChe*, Release 6.1.10; Fujitsu Ltd.: Miahama-Ku, Chiba City, Chiba, Japan, 2000−2003.
(20) Birks, J. B. *Photophysics of Aromatic Molecules*; Wiley: London, 1970.
(21) Zerner, M. C.; Loew, G. H.; Kirchner, R. F.; Mueller-Westerhoff, U. T. *J. Am. Chem. Soc.* **1980**, *102*, 589−599.

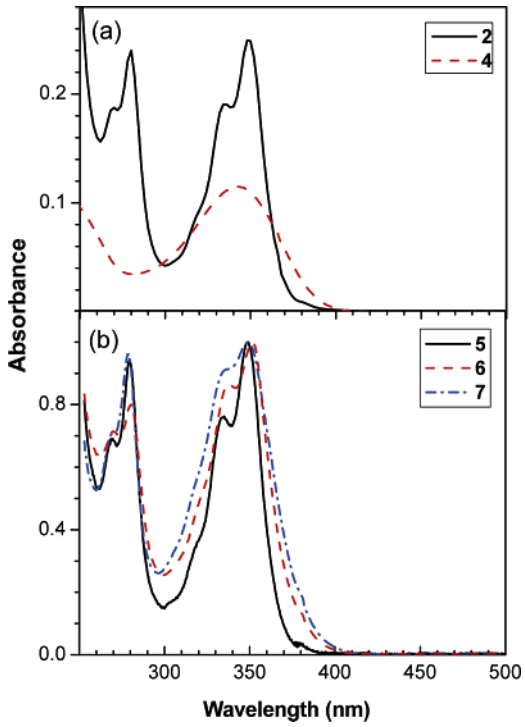

Figure 2. Ultraviolet absorption spectra of (a) ureas **2** and **4** and (b) ureas **5**−**7** (10 μM in MTHF).

Table 1. UV Absorption, Fluorescence, and Phosphorescence Data for Arylureas **1**−**7**[a]

urea	λ_{abs}, nm[b]	log ϵ[b]	λ_{fl}, nm[c]	Φ_{fl}[c]	τ_s, ns[c]	λ_{fl}, nm[d]	Φ_{fl}[d]	λ_p, nm[e]
1[f]	348		390	0.41	21.0	378	0.73	
2[f]	348	4.4	392	0.43	25.5	382	0.80	
3	354	4.0						490
4[g]	342	4.1						490
5	349	4.5	385	0.003		500	0.08	610
6	349	4.5	383	0.005		500	0.02	490
						382	0.03	610
7	352	4.5	392	0.007		500	0.02	490
			537	0.003		380	0.03	610

[a] All spectral data were obtained in MTHF solution. [b] Absorption maximum and absorbance data determined at 298 K. [c] Fluorescence maximum, quantum yield, and lifetime determined at 298 K. [d] Fluorescence maximum (ca. 380 nm for Py and 500 nm for CT fluorescence) and quantum yields determined at 77 K. [e] Phosphorescence 0,0 band (490 nm for NB and 610 nm for Py) and quantum yield determined at 77 K. [f] Data from ref 16. [g] Data from ref 18.

CAChe 6.1.10.[19] The calculated energy, absorbance, and character of selected low-energy singlet states of **2** and **4**−**7** are reported in Table 2, and their calculated absorption spectra and frontier orbitals are provided in the Supporting Information. The two lowest-energy transitions for **1** and **2** are assigned to pyrene π,π^* states (bands 1 and 2). The two lowest-energy transitions for **3**−**7** are assigned to nitrobenzene-localized n,π^* states with calculated energies corresponding to ca. 450 and 387 nm and low oscillator strengths. The lowest-energy allowed transition for **4** is a nitrobenzene-localized π,π^* state (S_4). These assignments are consistent with a previous calculation for nitrobenzene using the CAS-SCF method.[22] Two pyrene-localized $\pi-\pi^*$ transitions corresponding to pyrene bands 1 and 2 are calculated for **5**−**7**.[20] Other low-energy transitions for **4** and **5** are assigned to partially allowed charge-transfer (CT) states having phenyl → nitrobenzene (S_3 of **4**) or pyrene → nitrobenzene character (S_4 of **5**).

Table 2. Calculated Properties of Selected Singlet States of Ureas **2** and **4**−**7**[a]

urea	state	λ, nm	log ϵ, L mol^{-1} cm^{-1}	character[b]
2	S_1	367	3.0	Py π,π^*
	S_2	340	4.6	Py π,π^*
4	S_1, S_2	450, 387	0.3, 0.4	NB n,π^*
	S_3	318	3.5	CI
	S_4	309	4.4	NB π,π^*
5	S_1, S_2	449, 386	0.6, 0.6	NB n,π^*
	S_3	367	2.8	Py π,π^*
	S_4	353	3.7	CT
	S_5	338	4.5	Py π,π^*
6	S_1, S_2	449, 386	1.0, 0.3	NB n,π^*
	S_3	366	2.9	Py π,π^*
	S_4	338	4.6	Py π,π^*
7	S_1, S_2	449, 386	0.8, 0.3	NB n,π^*
	S_3	363	2.9	Py π,π^*
	S_4	337	4.6	Py π,π^*

[a] Wavelength, absorbance, and character based on in vacuo ZINDO calculations. [b] NB, nitrobenzene-localized state; Py, pyrene-localized state; CI, delocalized state with extensive configuration interaction; CT, Py→NB charge transfer.

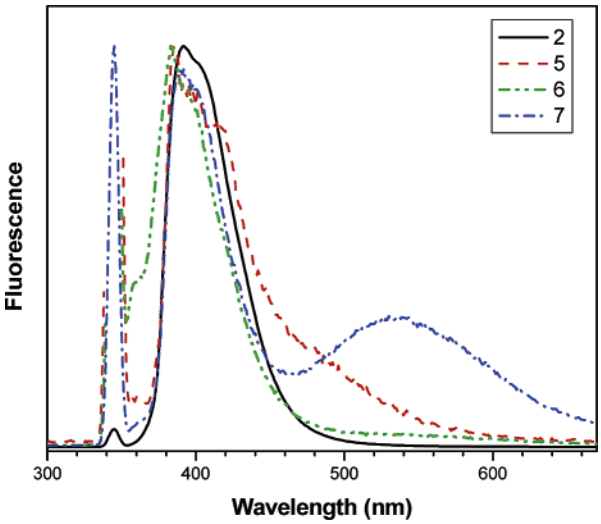

Figure 3. Fluorescence spectra of ureas **2** and **5**−**7** in MTHF solution at 298 K (345 nm peaks are scattered light).

Emission Spectra and Redox Potentials. The fluorescence spectra of the arylureas at room temperature in methyltetrahydrofuran (MTHF) solution are shown in Figure 3. Ureas **1** and **2** have strong fluorescence with quantum yields $\Phi_{fl} \approx 0.4$ and lifetimes $\tau = 21$ and 25 ns, respectively (Table 1). The quantum yields are similar to that of pyrene; however, the lifetimes are significantly shorter than that of pyrene (ca. 450 ns).[20] Ureas **3** and **4** are nonfluorescent at room temperature, as is the case for nitrobenzene and its derivatives.[23,24] The fluorescence spectra of **5**−**7** in MTHF at room temperature (Figure 3) have band maxima similar to those of **2**; however, additional features are observed at longer wavelengths. These appear as a shoulder for **5** and maxima near 540 nm for **6** (low intensity) and **7** (higher intensity). The quantum yields for

(22) Takezaki, M.; Hirota, N.; Terazima, M.; Sato, H.; Nakajima, T.; Kato, S. *J. Phys. Chem. A* **1997**, *101*, 5190−5195.
(23) Khalil, O. S.; Bach, H. G.; McGlynn, S. P. *J. Mol. Spectrosc.* **1970**, *35*, 455−460.
(24) Li, R.; Lim, E. C. *J. Chem. Phys.* **1972**, *57*, 605−612.

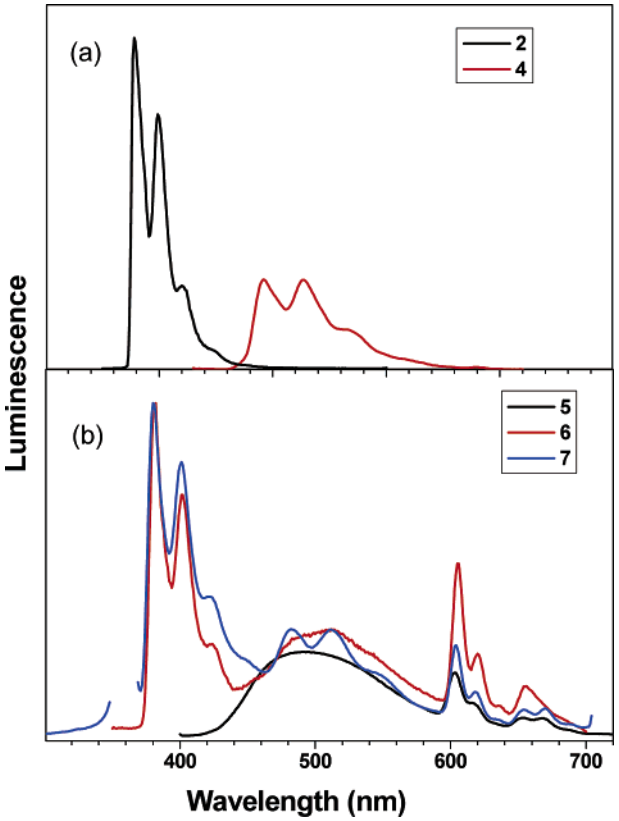

Figure 4. Luminescence spectra in MTHF solution at 77 K for (a) ureas **2** and **4** and (b) ureas **5**−**7**.

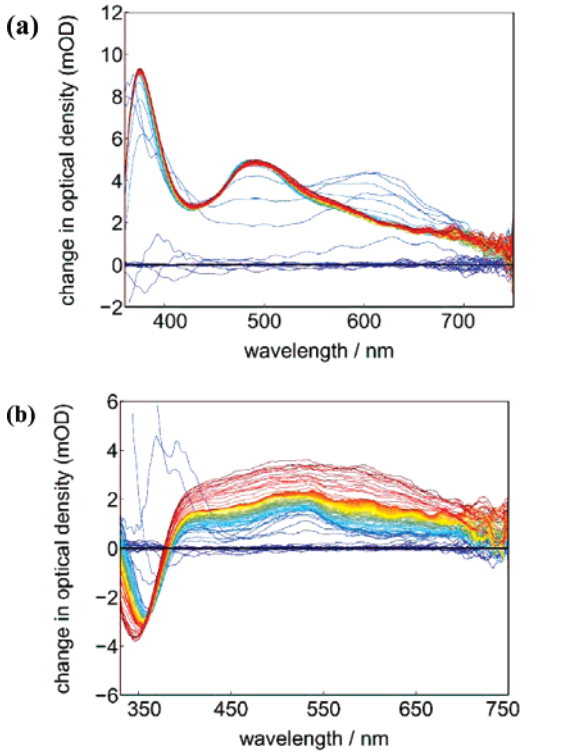

Figure 5. Temporal evolution of the pump−probe spectra of ureas (a) **2** and (b) **4** in the time range 0−10 ps following 346 nm excitation in THF. Early spectra are shown in blue/green colors and late spectra in orange/red colors.

fluorescence of **5**−**7** are ≤0.03, and their singlet lifetimes are ≤0.5 ns, the time resolution of our lifetime apparatus.

The total luminescence spectra of the arylureas **2** and **4**−**7** in MTHF glasses at 77 K are shown in Figure 4. The emission of **2** is similar to that of **1**, which has previously been reported and assigned to pyrene-localized fluorescence.[16] Both **1** and **2** have more structured fluorescence and somewhat higher values of Φ_{fl} at 77 K than at 298 K (Table 1). No phosphorescence is observed for either **1** or **2**. Both **3** and **4** are nonfluorescent at room temperature. The emission spectrum of **4** at 77 K has also been previously reported and attributed to nitrobenzene phosphorescence on the basis of its band shape and long decay time (0.4 s).[18]

The 77 K luminescence spectrum of **5** displays weak pyrene fluorescence and is dominated by a broad band centered at 490 nm which is not observed in the 77 K spectra of either **2** or **4**. Weaker structured emission is observed with a 0,0 band near 610 nm, assigned to pyrene phosphorescence on the basis of its wavelength and structure.[20] Slow warming of the 77 K glass results in a decrease in the intensity of both the 490 nm band and the 600 nm band. The latter is not observed above the MTHF glass transition temperature (ca. 120 K). The spectrum of **6** displays a structured 380 nm pyrene monomer band in addition to a broad band at 510 nm and a structured band at 610 nm attributed to pyrene phosphorescence. The spectrum of **7** is similar to that of **6**, except for the increased structure of the 500 nm band.

The oxidation and reductions potentials of ureas **1** and **4** were determined by cyclic voltametry in acetonitrile solution using ferrocene as an internal potential reference. The reversible reduction of **4** has a half-wave potential of −1.20 V vs SCE, less negative than the reported value for nitrobenzene (−1.65 V).[25] Urea **1** has irreversible reduction and oxidation waves with potentials of −2.00 and 1.33 V, respectively, vs SCE. The corresponding values for pyrene are −2.09 and 1.28 V vs SCE.[26]

Femtosecond Pump−Probe Spectra. Femtosecond time-resolved transient absorption spectra with a spectral range of 350−750 nm have been measured for ureas **1**−**7** in tetrahydrofuran (THF) and acetonitrile (MeCN). Spectra were obtained at time intervals between 0 and 1900 ps using a Ti:sapphire-based system with a time resolution of ca. 100 fs and a spectral resolution of ca. 5−7 nm. The spectra of **2** and **4**−**7** in THF are shown in Figures 5 and 6. Spectra obtained in MeCN (data not shown) are similar in appearance (band shape and maxima) to those obtained in THF but display differences in kinetics. The spectra of **1** and **3** (data not shown) are similar to those of **2** and **4**, respectively, in both solvents. Spectral assignments are discussed below, and kinetic data for **5**−**7** are summarized in Table 3.

The spectra of **2** obtained during the time interval 0−10 ps in THF are shown in Figure 5a. A long-wavelength band at 600 nm, assigned to pyrene S_2, rises during the laser pulse. Its decay is accompanied by a rise in the 490 nm band, assigned to pyrene S_1, which occurs with a rise time of ca. 100 fs. No change in band shape or intensity is observed during the ensuing 2 ns. The assignment of the 370 and 490 nm bands and the longer-wavelength shoulder to the pyrene S_1 state is consistent with previous assignments for pyrene and with the high fluorescence quantum yield and long singlet decay time for **2**

(25) Goodnow, T. T.; Kaifer, A. E. *J. Phys. Chem.* **1990**, *94*, 7682−7683.
(26) Kubota, T.; Kano, K.; Uno, B.; Konse, T. *Bull. Chem. Soc. Jpn.* **1987**, *60*, 3865−3877.

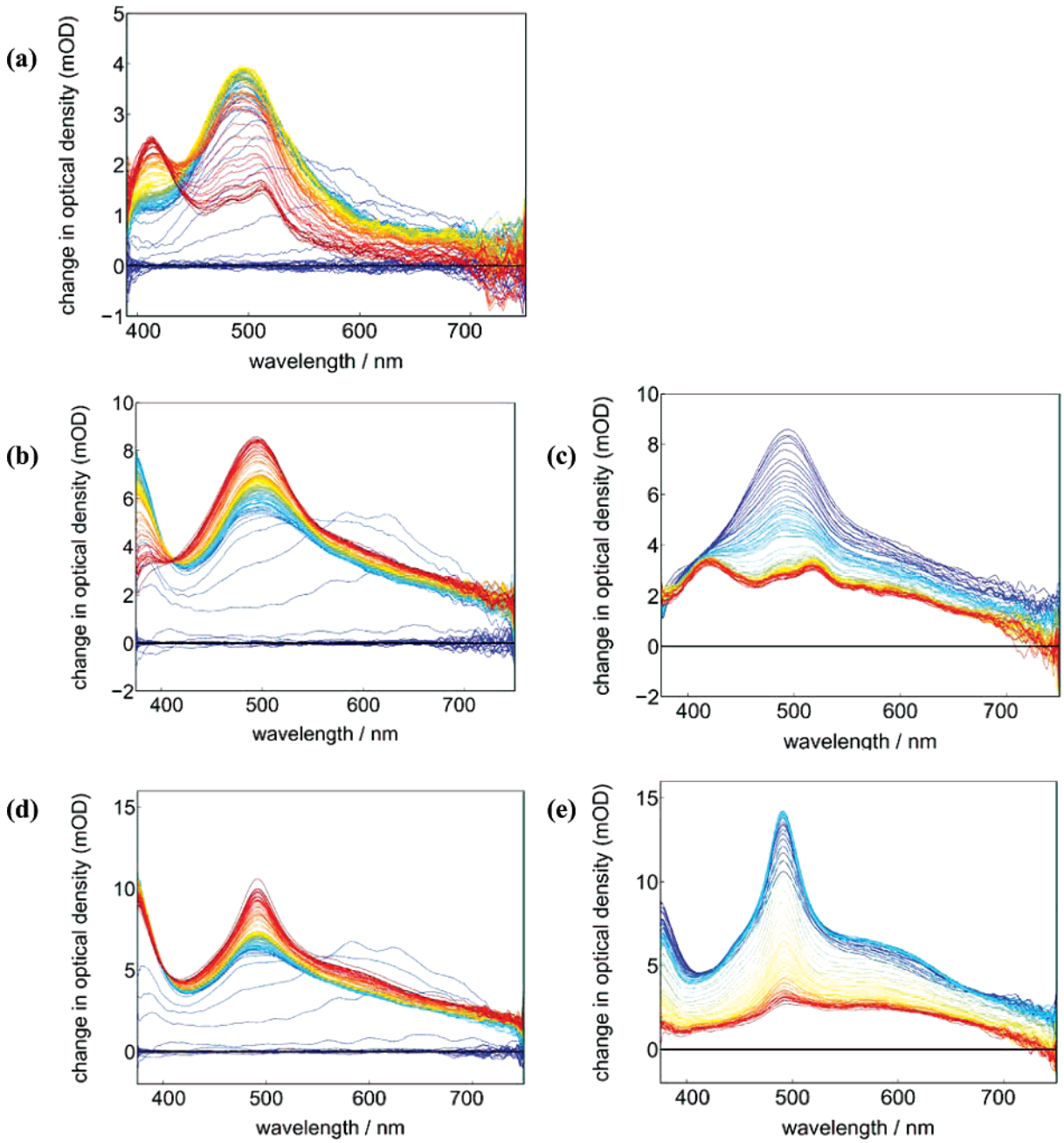

Figure 6. Pump−probe spectra of ureas **5** (a, 0−100 ps), **6** (b, 0−20 ps; c, 20−2000 ps), and **7** (d, 0−20 p; e, 20−2000 ps) in the indicated time ranges following 346 nm excitation in THF. Early spectra are shown in blue/green colors and late spectra in orange/red colors.

(Table 1).[27−30] The appearance and dynamics of the transient spectra of **1** are identical to those of **2**, and both spectra are similar in MeCN and THF.

The spectra of **4** in THF solution obtained during the time interval 0−10 ps are shown in Figure 5b. Positive bands at 390 and 530 nm rise during the laser pulse. These bands decay rapidly and are replaced by a sharp negative band at 340 nm and a broad positive band extending from 400 to beyond 750 nm. Both the 340 nm and long-wavelength bands gain intensity during the first several picoseconds and decay slowly. Fitting of the 415 or 470 nm transient absorption intensity provides rise times of ca. 10 ps for ureas **3** and **4** in both THF and MeCN solution (Table 3). The decay times are estimated to be similar to the experimental time window, ca. 2 ns. The fast rise time, broad spectrum, slow decay, and absence of solvent dependence are consistent with intersystem crossing to form the nitrobenzene triplet state.[31]

The spectra of **5** in THF (Figure 6a) display rise and decay of a 600 nm band during the laser pulse followed by growth of a broad band at 495 nm and a weaker band at 420 nm. The 495 nm maximum rises with a time constant of ca. 100 fs in both THF and MeCN, similar to the instrument time resolution. The

(27) Grellman, K. H.; Watkins, A. R.; Weller, A. *J. Phys. Chem.* **1972**, *76*, 469−473.
(28) Shafirovich, V. Y.; Levin, P. P.; Kuzmin, V. A.; Thorgeirsson, T. E.; Kliger, D. S.; Geacintov, N. E. *J. Am. Chem. Soc.* **1994**, *116*, 63−72.
(29) Foggi, P.; Pettini, L.; Santa, I.; Righini, R.; Califano, S. *J. Phys. Chem.* **1995**, *99*, 7439−7345.
(30) Raytchev, M.; Pandurski, E.; Buchvarov, I.; Modrakowski, C.; Fiebig, T. *J. Phys. Chem. A* **2003**, *107*, 4592−4600.
(31) Yip, R. W.; Sharma, D. K.; Giasson, R.; Gravel, D. *J. Phys. Chem.* **1984**, *88*, 5770−5772.

Table 3. Femtosecond Pump−Probe Transient Data for Ureas **4**−**7**[a]

urea	solvent	λ, nm	τ, ps	λ, nm	τ, ps
4	THF	415	12 (r, ^{3}NB)	570	11 (r, ^{3}NB) ≥1 ns (d, ^{3}NB)
	MeCN	415	8.5 (r, ^{3}NB)	550	8.9 (r, ^{3}NB) ≥1 ns (d, ^{3}NB)
5	THF			495	0.09 (r, $PY^{+\bullet}$)[b] 33 (d, $PY^{+\bullet}$) ≫1 ns (d, ^{3}Py)
	MeCN			495	0.08 (r, $PY^{+\bullet}$) 1.5 (d, $PY^{+\bullet}$) ≫1 ns (d, ^{3}Py)
6	THF			495	4.5 (r, $PY^{+\bullet}$) 73 (d, $PY^{+\bullet}$) ≥1 ns (d, ^{3}NB)
	MeCN			495	0.78 (r, $PY^{+\bullet}$) 11 (d, $PY^{+\bullet}$) ≥1 ns (d, ^{3}NB)
7	THF	380	23 (d, $Py^{-\bullet}$) 480 (d, $Py^{-\bullet}$)	490	23 (r, $Py^{-\bullet}$) 450 (d, $Py^{-\bullet}$) ≥1 ns (d, ^{3}NB)
	MeCN	380	18 (d, $Py^{-\bullet}$) 460 (d, $Py^{-\bullet}$)	490	23 (r, $Py^{-\bullet}$) 450 (d, $Py^{-\bullet}$) ≥1 ns (d, ^{3}NB)

[a] r, rising components; d, decaying components. [b] A second decay component with $\tau = 0.86$ ps is also observed and accounts for <10% of the total rising signal.

495 nm band then decays with a time constant of 33 ps in THF and 1.5 ps in MeCN, leaving a spectrum with maxima at 410 and 520 nm, which do not decay appreciably during the ensuing 2 ns. The 495 nm band is attributed to the $Py^{+\bullet}/NB^{-\bullet}$ CT state. It is broader and red-shifted when compared to the solution absorption spectrum of $Py^{+\bullet}$.[27,28,32] Shida reports absorption band maxima at 449 nm for $Py^{+\bullet}$ and 475 and 515 nm for $NB^{-\bullet}$ in low-temperature glasses.[33] The rapid formation of the CT state is consistent with the very weak fluorescence of **5**. The structured spectrum observed at longer delay times is identical to the spectrum of triplet pyrene.[32] The weak absorbance at wavelengths between 600 and 700 nm at long delay times indicates that little or no NB triplet is present.

The transient spectra of **6** in THF (Figure 6b,c) display a fast rise and decay of a 600 nm band, similar to those for **2** and **5**. The decay is accompanied by an initial rise in a broad, nonsymmetrical 500 nm band attributed to ^{1}Py, followed by a slower rise in the symmetrical 500 nm band attributed to $Py^{+\bullet}/NB^{-\bullet}$, which occurs with a time constant of 4.5 ps in THF and 0.78 ps in MeCN. The 500 nm band decays with time constants of 73 and 11 ps in THF and MeCN, respectively, leaving a long-lived transient having structure similar to that of triplet Py, superimposed on a broad spectrum assigned to triplet NB. The latter transient has a decay time similar to the 2 ns time window.

The transient spectra of **7** (Figure 6d,e) also display a fast rise and decay of the 600 nm pyrene S_2 band, accompanied by the rise of absorption maxima at 370 and 490 nm, similar to those of **2** and **6**, assigned to the formation of pyrene S_1. This is followed by decay of the 370 nm band and the rise of a relatively narrow 480 nm band, which occurs with time constants of ca. 20 ps in both THF and MeCN. This spectrum is assigned to the pyrene anion radical on the basis of its similarity to the spectrum of $Py^{-\bullet}$ formed upon inter- or intramolecular oxidation of aniline derivatives.[28,34] The 480 nm band and 575 nm shoulder decay with a time constant of 450 ps in THF and MeCN, leaving the broad spectrum of a long-lived transient assigned to triplet NB.

Discussion

The tertiary ureas **5**−**7** were designed to probe electronic interactions in π-stacked donor−bridge−acceptor systems possessing pyrene (Py) donor and nitrobenzene (NB) acceptor chromophores separated by 0−2 bridging phenylenediamine rings (B). Pyrene has been widely used as both donor and acceptor in studies of inter- and intramolecular electron transfer.[27,28,34,35] The selection of NB as the acceptor for these studies was based upon its low oxidation potential and ease of incorporation into the donor−acceptor diarylurea structure.[18,36] We note that NB has not been widely used as an acceptor in photoinduced electron transfer reactions, presumably because of its low singlet energy and rapid intersystem crossing (vide infra). Since Py and NB have overlapping absorption bands (Figure 2), elucidation of the excited-state behavior of ureas **1**−**4** is a prerequisite for interpretation of both the steady-state and femtosecond pump−probe spectra of the donor−acceptor ureas **5**−**7**. The transient absorption spectra of both Py and NB obtained with picosecond time resolution have previously been reported.[29−31,37] The femtosecond data obtained in the present study provides information about the internal conversion process in both chromophores and the intersystem crossing of NB, as well as the dynamics of electron transfer in π-stacked donor−bridge−acceptor systems.

The interchromophoric interaction of singlet Py with NB might occur via either singlet energy transfer or an electron-transfer mechanism. Whereas the singlet energy of the NB allowed π,π* state is higher than that of the Py singlet, NB dark states are predicted to lie below the Py S_1 singlet state on the basis of semiempirical ZINDO calculations (Table 2) as well as ab initio calculations.[22] The free energy of electron transfer from singlet Py to NB can be estimated from the singlet energy ($E_S = 3.27$ eV from the 0,0 band of the fluorescence spectrum) and oxidation potential ($E_{ox} = 1.09$ V vs SCE) of **1** and the NB reduction potential of **4** ($E_{rdn} = -1.20$ V vs SCE) using Weller's equation (eq 1), where the final term is an empirical

$$\Delta G_{et} = -E_s - (E_{rdn} - E_{ox}) + (2.6/\epsilon - 0.13\ \text{eV}) \quad (1)$$

correction for the solvent-dependent Coulomb attraction between the radical ions formed in the electron-transfer process (+0.21 eV for THF and −0.06 eV for MeCN).[38] Values of ΔG_{et} estimated for THF and MeCN are −0.77 and −1.04 eV, respectively. The NB singlet energy obtained from the ZINDO calculation (Table 2) is 2.76 eV, substantially lower than the value for Py but sufficiently large to drive the oxidation of ground-state Py.

Pyrenylureas. The presence of the tertiary urea substituents in **1** and **2** results in a red shift of their absorption and

(32) Okada, T.; Karaki, I.; Matsuzawa, E.; Mataga, N.; Sakata, Y.; Misumi, S. *J. Phys. Chem.* **1981**, *85*, 3957−3960.
(33) Shida, T. *Electronic absorption spectra of radical ions*; Elsevier: Amsterdam, 1988.
(34) Okada, T.; Migita, M.; Mataga, N.; Sakata, Y.; Misumi, S. *J. Am. Chem. Soc.* **1981**, *103*, 4715−4720.
(35) Pandurski, E.; Fiebig, T. *Chem. Phys. Lett.* **2002**, *357*, 272−278.
(36) Lepore, G.; Migdal, S.; Blagdon, D. E.; Goodman, M. *J. Org. Chem.* **1973**, *38*, 2590−2594.
(37) Takezaki, M.; Hirota, N.; Terazima, M. *J. Phys. Chem. A* **1997**, *101*, 3443−3448.
(38) Weller, A. *Z. Phys. Chem. Neue Folg.* **1982**, *133*, 93−98.

Scheme 1. Excited-State Behavior of Ureas (a) **2** and (b) **4**, Determined from Pump−Probe Experiments (S_1 Decay Time for **2** from Fluorescence Decay)[a]

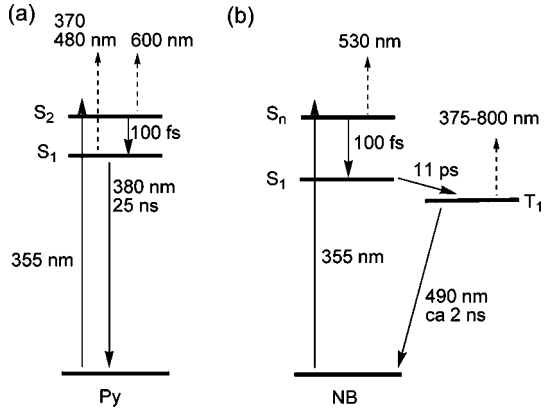

[a] Broken arrows indicate transient assignments.

fluorescence maxima (Table 1) relative to those of pyrene (334 and 372 nm, respectively).[20] The urea substituents are also responsible for a substantial decrease in the radiative lifetime ($\tau_{rad} = \tau_s/\Phi_{fl}$), from 950 ns for pyrene to 51 and 59 ns for **1** and **2**, respectively. The absorbances of the long-wavelength bands of **1** and **2** are stronger than that of pyrene, in accord with their shorter radiative lifetimes. The room-temperature fluorescence spectra of **1** and **2** (Figure 3) are broader than that of pyrene. Neither pyrenylurea is phosphorescent at 77 K in a MTHF glass (Figure 4). The observation of phosphorescence for pyrene but not for **1** and **2** may reflect the significantly longer pyrene singlet radiative lifetime. The reduction potential of **1** is less negative than that of pyrene (−2.00 vs −2.09 eV) and its oxidation potential more positive (1.33 vs 1.28 eV),[26] indicative of a weakly electron-donating effect of the tertiary urea substituent.

The transient absorption spectra of **1** and **2** (Figure 5) display a 600 nm band which rises during the pump pulse and decays with a time constant of ca. 100 fs. Its decay is accompanied by the rise of a spectrum with maxima at 370 and 480 nm, a shoulder near 575 nm, and a long-wavelength tail extending beyond 700 nm. This spectrum does not change band shape or decay appreciably during the 2 ns time window of the transient measurements. The band shape of this spectrum is similar to those previously reported for the S_1 state of pyrene; however, the maxima are red-shifted by ca. 20 nm relative to those of pyrene.[29,30] This assignment is consistent with the high fluorescence quantum yields and decay times of **1** and **2**, which are significantly longer than the 2 ns time window. The short-lived 600 nm band is assigned to pyrene S_2 absorption, in accordance with previous femtosecond broadband studies on the S_2-S_1 internal conversion dynamics in pyrene (and phenyl pyrene) by the Fiebig group.[30] The singlet-state behavior of the pyrenylureas is summarized in Scheme 1a. Excitation at 355 nm populates the allowed S_2 π,π^* state, which rapidly decays to the long-lived S_1 state.

Nitrophenylureas. The absorption and luminescence spectra of ureas **3** and **4** have recently been described.[18] To briefly summarize, their broad 348 nm absorption bands (Figure 2) are attributed by ZINDO calculations to an allowed $\pi-\pi^*$ transition and several lower-energy transitions (Table 2). Ureas **3** and **4**, like nitrobenzene, are nonfluorescent at room temperature. The absence of fluorescence has been attributed to rapid intersystem crossing from the lowest n,π^* singlet to the π,π^* triplet.[22,31,37] The strong, structured luminescence observed at 77 K (Figure 4) is assigned to ^{3}NB on the basis of a band shape which is similar to those of 4-nitroaniline and 4-nitrophenol.[39] The absence of phosphorescence from the parent nitrobenzene has been attributed to rapid triplet-state decay.[40] The reduction potential of **4** is −1.20 V vs SCE, less negative than the reported value for nitrobenzene (−1.65 V),[25] in accord with charge delocalization in the anion radical of **4**.

The transient absorption spectra of **3** and **4** (Figure 5b) display the rapid rise of a 530 nm band and decay of a 390 nm band. This is followed by the slower growth of a negative band at 340 nm (attributed to bleaching of the ground state) and of a broad absorption band extending from 375 to beyond 750 nm (attributed to the nitrobenzene triplet state). The rise time for this band is 11 ± 1 ps, similar to the values for ^{1}NB intersystem crossing estimated either by picosecond transient absorption spectroscopy (ca. 5 ps) or by the transient grating method (ca. 10 ps).[31,37] Yip et al. report a broad transient absorption band for ^{3}NB with a maximum near 650 nm and a second band near 450 nm.[31] The decay times for the transient absorption of triplets **3** and **4** are ca. 2 ns, similar to the time window of our measurements. Yip et al. report a decay time of 0.8 ns for triplet nitrobenzene in THF solution.[31] The photophysical behavior of the nitrophenylureas is summarized in Scheme 1b. The changes in the transient spectra which occur with a time constant of ca. 100 fs are attributed to rapid internal conversion from the initially formed π,π^* state to the lowest-energy n,π^* state. The rapid rate of intersystem crossing is consistent with conversion of an n,π^* singlet to a π,π^* triplet separated by a small energy gap, according to El-Sayed's rules.[41]

Donor−Acceptor Diarylurea 5. On the basis of the spectra of ureas **2** and **4**, the pyrene chromophore is expected to absorb about two-thirds of the 355 nm incident light in the pump−probe studies of the Py-NB ureas **5**−**7**. In accord with this expectation, the transient spectra of **5**−**7** at short delay times following the femtosecond excitation pulse are dominated by the spectrum of pyrene S_2 (Figure 6). In the case of **5**, excitation at 355 nm results in a rapid rise and decay of the pyrene S_2 600 nm band. The decay of S_2 is accompanied by a ca. 100 fs rise of a symmetric band at 495 nm assigned to the CT state $Py^{+\bullet}/NB^{-\bullet}$ (Table 1). Internal conversion from the pyrene S_2 state (which corresponds to the S_5 state of **5** in the ZINDO calculations, Table 2) directly to the CT state is indicative of strong coupling between these states and consistent with the low quantum yield for Py fluorescence both at room temperature and at 77 K (Table 1) and the appearance of a broad 500 nm band at 77 K in MTHF (Figure 4). Similar ultrafast internal conversion dynamics between the pyrene S_2 and a CT state has been observed in directly covalently linked pyrene−methyl benzoate systems.[35]

The 495 nm CT transient absorption band of **5** decays with time constants of 33 ps in THF and 1.5 ps in MeCN, consistent with the absence of strong CT steady-state fluorescence at room temperature (Figure 3). Its decay leaves a long-lived spectrum having a band structure similar to that of the pyrene triplet.[28,32] The rapid intersystem crossing from the singlet CT state to the

(39) Brinen, J. S.; Singh, B. *J. Am. Chem. Soc.* **1971**, *93*, 6623−6629.
(40) Kröhl, O.; Malsch, K.; Swiderek, P. *Phys. Chem. Chem. Phys.* **2000**, *2*, 947−953.
(41) El-Sayed, M. A. *J. Chem. Phys.* **1963**, *38*, 2834−2838.

Scheme 2. Excited-State Behavior of Ureas (a) **5**, (b) **6**, and (c) **7**[a]

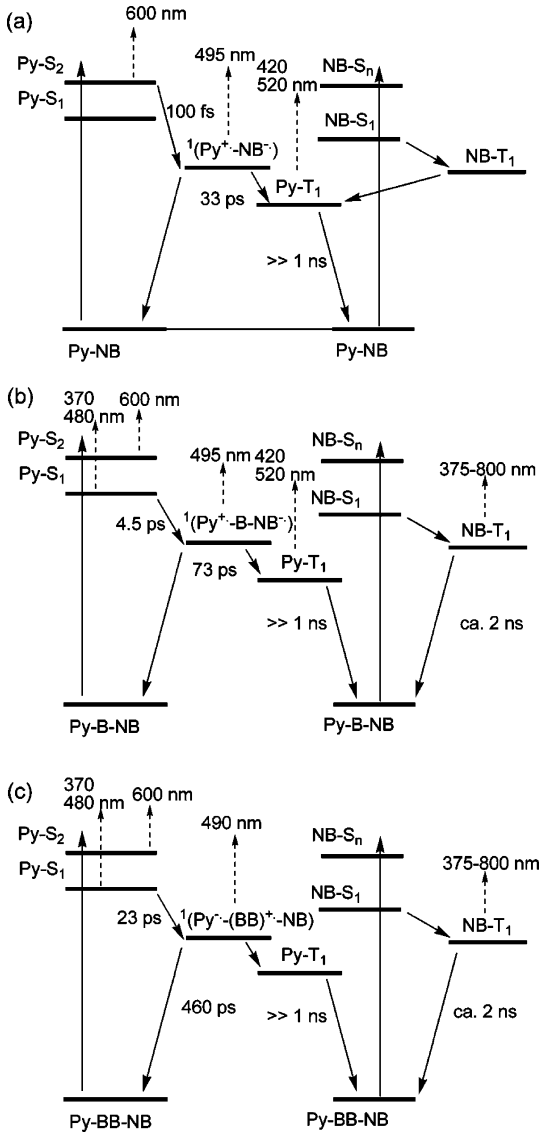

[a] Broken arrows indicate transient assignments.

pyrene triplet state might result from mixing with the low-energy NB n,π* states or out-of-plane urea n,π* states. The absence of the broad transient absorption characteristic of ^{3}NB is consistent with the lower energy of ^{3}Py-NB vs ^{3}NB-Py and the short Py-NB plane-to-plane separation, which should promote rapid intramolecular T−T transfer.[42] This proposal is supported by the observation of structured Py phosphorescence but not NB phosphorescence at 77 K (Figure 4).

The excited-state behavior of urea **5** in THF is summarized in Scheme 2a. Charge separation is attributed to internal conversion of the initially excited Py π,π* singlet state directly to the CT state. Similar ultrafast charge transfer was reported by Therien and co-workers for a cofacial porphyrin−quinone dyad and may be a characteristic of π-stacked donor−acceptor molecules with short plane-to-plane separations and low-lying CT states.[10] The CT state of **5** undergoes charge recombination with a 33 ps decay time in THF and 1.5 ps in MeCN, resulting in population of the ^{3}Py. The solvent effect is similar to that observed by Okada et al. for pyrene/aniline singlet CT states and attributed to a reduction in the energy gap for the charge recombination process in more polar solvents.[32] The absence of detectable ^{3}NB in either the transient or steady-state spectra (Figures 6a and 4b) indicates that direct excitation of NB results in population of either ^{3}PY or the CT singlet state.

Donor−Bridge−Acceptor Diarylurea 6. As is the case for the pyrenylureas **2** and **5**, pulsed laser excitation of **6** in THF (Figure 6b) results in the rapid rise and decay of the 600 nm Py S_2 band. Its decay occurs with a time constant of ca. 100 fs and is accompanied by the growth of 370 and 480 nm bands assigned to Py S_1. This is followed by a rise and narrowing of a 495 nm band attributed to formation of the $Py^{+\bullet}-B-NB^{-\bullet}$ CT state, which occurs with time constants of 4.5 and 0.78 ps in THF and MeCN, respectively. The stronger 77 K Py fluorescence for **6** vs **5** (Table 1) is consistent with slower charge separation for **6**.

The 495 nm band CT of **6** decays with time constants of 73 and 11 ps in THF (Figure 6c) and MeCN, respectively, attributed to charge recombination of the CT state. The CT state may be responsible for the weak, broad emission observed near 550 nm in the 298 K fluorescence spectrum and the stronger band near 500 nm in the 77 K luminescence spectra of **6** (Figures 3 and 4). Decay of the 495 nm CT band leaves a long-lived transient with absorption extending from 400 to 800 nm, assigned to a superposition of the structured ^{3}Py and unstructured ^{3}NB absorption bands (compare Figures 6c and 5b). This assignment is consistent with the 77 K luminescence spectrum of **6**, which displays both a structured 605 nm ^{3}Py band and a weakly structured 490 nm ^{3}NB band which is superimposed on the broad CT luminescence.

The excited-state behavior of urea **6** in THF is summarized in Scheme 2b. Following Py $S_2 \rightarrow S_1$ internal conversion, electron transfer from ^{1}Py to NB results in the formation of the $Py^{+\bullet}-B-NB^{-\bullet}$ CT state with a time constant of ca. 4.5 ps. Since reduction of the bridging phenylenediamine is expected to be highly endergonic,[43] charge separation most likely occurs via a single-step superexchange mechanism. The decay of the CT state occurs with a time constant of 73 ps in THF, somewhat slower than the 33 ps time constant for decay of the CT state of **5**. Both the formation and decay of the CT state are faster in MeCN than in THF, in accord with a larger driving force for photoinduced charge transfer (Marcus normal region behavior) and a smaller driving force for charge recombination (Marcus inverted region behavior) in the more polar solvent.[44] The weak ^{3}NB transient absorption observed at long delay times (Figure 6c) most likely arises from ^{1}NB intersystem crossing. The band shape for the transient spectrum of **6** does not change appreciably between 0.2 and 2 ns. Thus, T−T energy transfer between NB and Py evidently does not occur on this time scale, in accord with the strong distance dependence for this spin-forbidden process.[42]

Donor−Bridge−Acceptor Diarylurea 7. As is the case for ureas **2**, **5**, and **6**, pulsed laser excitation of **7** results in the formation of the Py S_1 state via $S_2 \rightarrow S_1$ internal conversion with a decay time of ca. 100 fs (Figure 6d). Decay of the Py S_1

(42) Turro, N. J. *Modern Molecular Photochemistry*; Benjamin/Cummings: Menlo Park, CA, 1978.
(43) Lewis, F. D.; Kurth, T. L.; Delos Santos, G. *J. Phys. Chem. B* **2005**, *109*, 4893−4899.
(44) (a) Marcus, R. A. *J. Chem. Phys.* **1956**, *24*, 966−978. (b) Marcus, R. A. *J. Chem. Phys.* **1965**, *43*, 679−701.

380 nm band is accompanied by the rise of a narrow band at 490 nm with a shoulder at 600 nm. The 380 nm decay and the 490 nm rise have time constants of 23 ps in both THF and MeCN (Table 3). The slower S_1 decay for **7** vs **5** or **6** is consistent with its stronger fluorescence at 298 K (Table 1). The appearance of the transient spectrum of **7** at 20 ps (Figure 6d) is distinct from the spectra of the CT states of **5** and **6**. The lack of solvent dependence for the formation and decay of the 490 nm band of **7** also differentiates the behavior of **7** from those of **5** and **6**. The 490 nm band of **7** is assigned to $Py^{-\bullet}$ on the basis of its appearance, which is similar to that of the transient observed by Okada et al. for the intramolecular CT state formed upon excitation of a linked pyrene−dimethylaniline system ($Py^{-\bullet}/DMA^{+\bullet}$) in acetone.[34]

The free energy for formation of the $Py^{-\bullet}B^{+\bullet}$ contact radical ion pair can be calculated using Weller's equation (eq 1), the singlet energy (3.27 eV) and ground-state reduction potential (−2.00 V vs SCE) of the model urea **1**, and the oxidation potential of the bridging phenylenediamine ring. We have reported a decrease in the oxidation potential from 1.12 to 0.86 V, respectively, for polyphenylureas with one vs two bridging phenylenediamines.[43] The decreased oxidation potential is attributed to hole delocalization over two vs one interior phenylenediamines. A similar dependence of oxidation potential upon the extent of stacking has been reported for poly(dibenzofulvene).[45] Using the potentials for the polyphenylureas and eq 1, values of $\Delta G_{et} = -0.20$ and $+0.06$ eV are calculated for photooxidation of the bridging phenyls of **7** and **6**, respectively, in THF. These values are consistent with the occurrence of bridge oxidation for **7** but not for **6**.

Decay of the 490 nm transient for **7** occurs with a time constant of 450 ps, leaving a broad, long-lived transient assigned to triplet NB (Figure 6e). The relatively long decay time for the CT state can account for the observation of stronger room-temperature CT fluorescence for **7** than for either **5** or **6** (Figure 3). The absence of the structured transient absorption characteristic of ^{3}Py indicates that charge recombination of the CT state is dominated by return to the ground state rather than population of the triplet state. Neither does T−T energy transfer from the ^{3}NB triplet to Py occur during the 2 ns time window of the transient measurements, presumably due to the relatively large distance between the Py and NB chromophores. Weak ^{3}Py and ^{3}NB phosphorescence (the latter superimposed on the broad CT emission) is observed at 77 K (Figure 4b).

The excited-state behavior of **7** in THF is summarized in Scheme 2c. Following $S_2 \rightarrow S_1$ internal conversion, electron transfer from the bridging phenylenediamines to ^{1}Py generates the $Py^{-\bullet}/(BB)^{+\bullet}$ CT state. Charge separation and charge recombination occur with time constants of 23 and 450 ps, which are essentially independent of solvent polarity and are substantially slower than those for ureas **5** or **6**. The lack of solvent dependence may reflect both delocalization of the cation over two bridging phenylenediamines and the protection of their π-faces from solvation by π-stacking with Py and NB. Charge separation is slower than NB intersystem crossing in **4**; thus, singlet NB most likely decays via intersystem crossing rather than charge separation. The absence of the characteristic ^{3}Py absorption band at 410 nm in the transient spectra indicates that neither intersystem crossing of the singlet CT state nor T−T energy transfer from triplet NB occurs to an appreciable extent.

Concluding Remarks. Each of the three π-stacked pyrene−nitrobenzene systems **5**−**7** undergoes photoinduced charge separation; however, the mechanism and dynamics of the CT process are highly dependent upon the presence or absence of the bridging phenylenediamines. The highly idiosyncratic behavior of the donor acceptor ureas **5**−**7** illustrates the complexities inherent in π-stacked donor−acceptor and donor−bridge−acceptor systems. Strong electronic interaction between the Py donor and NB acceptor in **5** results in ultrafast charge separation, which is best described as an internal conversion process of the donor−acceptor system rather than charge separation between a locally excited acceptor and a ground-state donor.[35] A similar mechanism may account for the ultrafast formation of CT states upon excitation of other π-stacked systems with adjacent donor−acceptor pairs, including the DNA hairpins that we and others have investigated.[6]

The behavior of urea **6** presents the only case of bridge-mediated superexchange electron transfer in this series of ureas. The time constants for charge separation and charge recombination in THF (Table 3) are remarkably similar to those for superexchange electron transfer in a DNA hairpin possessing a stilbenedicarboxamide acceptor and guanine donor separated by a single A:T base pair (4 ps for charge separation and 94 ps for charge recombination).[46] Even faster time constants are observed for charge separation and charge recombination of **6** in MeCN.

The behavior of urea **7** is unique in that the role of pyrene is reversed from that of an electron donor to that of an electron acceptor, the bridging phenylenediamines serving as the electron donor. This role reversal reflects both lowering of the bridge oxidation potential upon addition of a second internal bridging unit and the anticipated decreased rate constant for strongly distant-dependent Py/NB superexchange electron transfer.[47] Unlike the behavior of **6**, the dynamics of charge separation and charge recombination of **7** are independent of solvent polarity. The interior phenylenediamine donors in **7**, like the interior base pairs in DNA, do not have their charged surfaces exposed to the solvent. The behavior of **7** suggests that Py−$(B)_n$−D systems, where $(B)_n$ is a series of phenylenediamine urea linkers and D is a hole trap, may provide a good model system for the study of bridge-mediated hole hopping and hole trapping.

Experimental Section

General Methods. ^{1}H NMR spectra for methylated compounds were measured at 400 or 500 MHz in $CDCl_3$ solution with TMS as internal standard. Chemical shifts (δ) are quoted in parts per million. *J* values are given in hertz. UV−vis spectra were measured on a diode array spectrometer using a 1 cm path length quartz cell. Low-temperature spectra emissions were measured either in a Suprasil quartz EPR tube (i.d. = 3.3 mm) using a quartz liquid nitrogen coldfinger Dewar at 77 K or in a nitrogen-cooled cryostat. Total emission quantum yields were measured by comparing the integrated area under the total emission curve at an equal absorbency and the same excitation wavelength as an external standard, 9,10-diphenylanthracene ($\Phi_{fl} \approx 1.0$ at 77 K in

(45) Nakano, T.; Yade, T. *J. Am. Chem. Soc.* **2003**, *125*, 15474−15484.

(46) Lewis, F. D.; Wu, T.; Liu, X.; Letsinger, R. L.; Greenfield, S. R.; Miller, S. E.; Wasielewski, M. R. *J. Am. Chem. Soc.* **2000**, *122*, 2889−2902.

(47) Lee, M.; Shephard, M. J.; Risser, S. M.; Priyadarshy, S.; Paddon-Row, M. N.; Beratan, D. N. *J. Phys. Chem. A.* **2000**, *104*, 7593−7599.

MTHF).[24] Emission spectra are uncorrected, and the estimated error for the quantum yields is ±10%. Phosphorescence decays were measured on a time-based detection instrument excited with a xenon flash lamp as the excitation source. Nonlinear least-squares fitting of the decay curves employed the Levenberg−Marquardt algorithm as described by James et al.[48] and implemented by the Photon Technologies International Timemaster (version 1.2) software. Goodness of fit was determined by judging the χ^2 (<1.3 in all cases), the residuals, and the Durbin−Watson parameter (>1.6 in all cases). Solutions were degassed under vacuum (<0.1 Torr) through five freeze−pump−thaw cycles.

Ground-state structures were optimized with the AM1 method implemented in MOPAC as implemented in CAChe 6.1.10.[19] Electronic structure calculations were performed on a PC with the ZINDO Hamiltonian (26 occupied and 26 unoccupied orbitals) as implemented in CAChe 6.1.10.

Materials. Triphosgene, triethylamine, aniline, 4-nitroaniline, 1-aminopyrene, and 1,4-phenylenediamine are commercially available and used as received. Anhydrous MTHF containing 200 ppm BHT was distilled over sodium under a nitrogen atmosphere. The synthesis and characterization of **1**, **3**, and **4** have previously been reported. The pyrene−nitrophenylureas were synthesized by the methods previously reported for the corresponding naphthyl−phenylureas and characterized by ^{1}H NMR and elemental analysis.[17,18]

1,3-Dimethyl-1-pyren-1-yl-3-(4-nitrophenyl)urea (2): mp 121−122 °C; ^{1}H NMR ($CDCl_3$, 400 MHz) δ 3.14 (s, 3H), 3.45 (s, 3H), 6.42 (d, 2H), 6.48 (t, 1H), 6.68 (d, 2H), 7.35 (d, 2H), 7.80 (d, 1H), 7.88 (d, 2H), 7.95 (m, 2H), 8.10 (d, 2H). Anal. Calcd for $C_{25}H_{20}N_2O$: C, 82.39; H, 5.53; N, 7.69. Found: C, 82.18; H, 5.67; N, 7.72.

1,3-Dimethyl-1-pyren-1-yl-3-(4-nitrophenyl)urea (5): mp 146−148 °C; ^{1}H NMR ($CDCl_3$, 400 MHz) δ 3.10 (s, 3H), 3.55 (s, 3H), 6.72 (d, J = 6.8, 2H), 7.47 (d, J = 6.4, 1H), 7.62 (d, J = 7.2, 2H), 7.90 (d, J = 6.4, 1H), 7.96 (d, J = 7.2, 2H), 8.07 (m, 2H), 8.14 (d, J = 7.2, 1H), 8.23 (m, 2H). Anal. Calcd for $C_{25}H_{19}N_3O_3$: C, 73.34; H, 4.68; N, 10.26. Found: C, 73.15; H, 4.80; N, 10.20.

1-[4-(3-Naphthalen-1-yl-ureido)phenyl]-1,3-dimethyl-3-(4-nitrophenyl)urea (6): ^{1}H NMR (DMSO-d_6, 400 MHz) δ 7.43 (d, J = 8.8, 2H), 7.50 (d, J = 8.8, 2H), 7.68 (d, J = 9.2, 2H), 8.05 (d, J = 8.4, 2H), 8.11 (d, J = 9.2, 1H), 8.18 d, J = 8.8, 2H), 8.24 (m, 4H), 8.35 (d, J = 9.2, 1H), 8.63 (d, J = 8.4, 1H), 8.84 (s, 1H), 9.08 (s, 1H), 9.16 (s, 1H), 9.41 (s, 1H).

1-[4-(1,3-Dimethyl-3-pyren-1-yl-ureido)phenyl]-1,3-dimethyl-3-(4-nitrophenyl)urea (7): mp 232−234 °C; ^{1}H NMR ($CDCl_3$, 400 MHz) δ 2.14 (s, 3H), 2.48 (s, 3H), 3.08 (s, 3H), 3.41 (s, 3H), 5.98 (d, J = 8.4, 2H), 6.30 (d, J = 8.4, 2H), 6.59 (d, J = 9.2, 2H), 7.54 (d, J = 8.0, 1H), 7.80 (m, 3H), 7.91 (m, 2H), 7.99, (m, 3H), 8.13 (m, 2H). Anal. Calcd for $C_{34}H_{29}N_5O_4$: C, 71.44; H, 5.11; N, 12.25. Found: C, 71.83; H, 5.23; N, 12.09.

Urea 6b: ^{1}H NMR (DMSO-d_6, 500 MHz) δ 7.41 (m, 6H), 7.47 (d, J = 9.0, 2H), 7.69 (d, J = 9.0, 2H), 8.05 (m, 2H), 8.12 (d, J = 9.0, 1H), 8.19 (d, J = 9.0, 2H), 8.26 (m, 4H), 8.36 (d, J = 9.5, 1H), 8.53 (m, 2H), 8.64 (d, J = 8.5, 1H), 8.79 (s, 1H), 9.02 (s, 1H), 9.14 (s, 1H), 9.39 (s, 1H).

Urea 6a: ^{1}H NMR ($CDCl_3$, 500 MHz) δ 1.95 (s, 3H), 2.63 (s, 3H), 3.06 (m, 6H), 3.10 (s, 3H), 3.41 (s, 3H), 5.85 (d, J = 8.5, 2H), 6.16 (d, J = 8.5, 2H), 6.28 (d, J = 8.5, 2H), 6.42 (d, J = 8.5, 2H), 6.86 (d, J = 9.0, 2H), 7.48 (d, J = 8.0, 1H), 7.76 (d, J = 9.0, 1H), 7.89 (m, 5H), 7.97 (d, J = 9.0, 2H), 8.13 (m, 2H); MS m/z 733.3 ($M^{+\bullet}$).

Femtosecond Broadband Pump−Probe Spectroscopy. A detailed description of our experimental setup has been given elsewhere.[30] The pump wavelength was set to 355 nm for all ureas. The changes in optical density were probed by a femtosecond white light continuum (WLC) generated by tight focusing of a small fraction of the output of a commercial Ti:sapphire-based pump laser (CPA-2010, Clark-MXR) into a 3 mm calcium fluoride (CaF_2) plate. The WLC provides a usable probe source between 300 and 750 nm. The WLC was split into two beams (probe and reference) and focused into the sample using reflective optics. After passing through the sample, both probe and reference beams were spectrally dispersed and simultaneously detected on a CCD sensor. The pump pulse (1 kHz, 400 nJ) was generated by frequency-doubling of the compressed output of a home-built NOPA system (from 666 to 708 nm respectively, 7 μJ, 40 fs). To compensate for group velocity dispersion in the UV pulse, an additional prism compressor was used. The overall time resolution of the setup is determined by the cross correlation function between pump and probe pulses, which is typically 100−120 fs (fwhm, assuming a Gaussian line shape). A spectral resolution of 5−7 nm was obtained. All measurements were performed with magic angle (54.7°) setting for the polarization of the pump with respect to the polarization of the probe pulse. A sample cell with 1.25 mm fused silica windows and an optical path of 1 mm was used for all measurements. A wire stirrer was used to ensure fresh sample volume was continuously used during the measurement.

Acknowledgment. Funding for this research was provided by National Science Foundation grants CHE-0100596 and CHE-0400663 (F.D.L.) and bilateral research grant AC1-3223 from the U.S. Civilian Research and Development Foundation (F.D.L. and S.A.M.) and Boston College (T.F.).

Supporting Information Available: ZINDO-calculated frontier orbitals, transitions, and absorption spectra for ureas **1** and **4**−**7**. This material is available free of charge via the Internet at http://pubs.acs.org.

JA058050X

(48) James, D. R.; Siemiarczuk, A.; Ware, W. R. *Rev. Sci. Instrum.* **1992**, *63*, 1710−1716.